Energies **2012**, *5*, 2112-2140; doi:10.3390/en5072112

OPEN ACCESS

energies

ISSN 1996-1073

www.mdpi.com/journal/energies

Article

Methane Production from Gas Hydrate Deposits through Injection of Supercritical CO_2

Christian Deusner *, Nikolaus Bigalke, Elke Kossel and Matthias Haeckel *

GEOMAR, Helmholtz Centre for Ocean Research Kiel, Wischhofstr.1-3, D-24148, Kiel, Germany; E-Mails: nbigalke@geomar.de (N.B.); ekossel@geomar.de (E.K.)

* Authors to whom correspondence should be addressed; E-Mails: cdeusner@geomar.de (C.D.); mhaeckel@geomar.de (M.H.); Tel.: +49-431-600-1415; Fax: +49-431-600-1400.

Received: 5 April 2012; in revised form: 5 May 2012 / Accepted: 7 June 2012 / Published: 25 June 2012

Abstract: The recovery of natural gas from CH_4-hydrate deposits in sub-marine and sub-permafrost environments through injection of CO_2 is considered a suitable strategy towards emission-neutral energy production. This study shows that the injection of hot, supercritical CO_2 is particularly promising. The addition of heat triggers the dissociation of CH_4-hydrate while the CO_2, once thermally equilibrated, reacts with the pore water and is retained in the reservoir as immobile CO_2-hydrate. Furthermore, optimal reservoir conditions of pressure and temperature are constrained. Experiments were conducted in a high-pressure flow-through reactor at different sediment temperatures (2 °C, 8 °C, 10 °C) and hydrostatic pressures (8 MPa, 13 MPa). The efficiency of both, CH_4 production and CO_2 retention is best at 8 °C, 13 MPa. Here, both CO_2- and CH_4-hydrate as well as mixed hydrates can form. At 2 °C, the production process was less effective due to congestion of transport pathways through the sediment by rapidly forming CO_2-hydrate. In contrast, at 10 °C CH_4 production suffered from local increases in permeability and fast breakthrough of the injection fluid, thereby confining the accessibility to the CH_4 pool to only the most prominent fluid channels. Mass and volume balancing of the collected gas and fluid stream identified gas mobilization as equally important process parameter in addition to the rates of methane hydrate dissociation and hydrate conversion. Thus, the combination of heat supply and CO_2 injection in one supercritical phase helps to overcome the mass transfer limitations usually observed in experiments with cold liquid or gaseous CO_2.

Keywords: gas hydrates; methane; energy; carbon dioxide; CCS

1. Introduction

Large amounts of natural gas, predominantly methane, are stored in gas hydrates in sediments below the seafloor and the permafrost [1]. Current estimates of the global methane hydrate inventory range between 1000 and 10,000 Gt of carbon [2–5]. Motivated by these results, gas hydrate research activities worldwide center around the exploitation of this potential new energy resource. The methods that are currently discussed to produce the methane from gas hydrates are generally derived from standard techniques used in conventional oil and gas business, *i.e.*, reduction of the pressure in the reservoir and thermal stimulation, as well as injection of hydrate inhibitors, such as salt, to induce dissociation of the gas hydrates [6]. In addition, the substitution of CH_4 by CO_2 as guest molecule in the gas hydrate structure has been proposed as a more elegant production technology with respect to greenhouse gas policies [7,8].

All of these methods have been studied in laboratory experiments to validate their feasibility as well as in numerical simulations to gain first ideas about their applicability on reservoir scale. First production tests were carried out in the permafrost reservoir of Mallik in northern Canada in 2002 [9] as well as in 2008 [10]. Gas hydrates were successfully destabilized by injection of hot water and by depressurization, respectively, producing limited amounts of CH_4 gas over a few days. Further field trials in 2012 will test the chemical exchange of methane in gas hydrates by injection of CO_2 below the permafrost of the Alaska North Slope [11] and the depressurization technique in the first offshore test in the Nankai Trough [12,13].

Overall, the conclusions drawn from those studies are that thermal stimulation by injecting hot water is slow and inefficient, whereas depressurization seems to be the more promising strategy [6]. However, due to the endothermic nature of gas hydrate dissociation, in the long run, the reservoir will cool down, re-establishing stable conditions for gas hydrates and consequently, methane production rates are expected to cease after some time [14,15].

Thus, being able to achieve stable and economic methane production rates will require a combination of depressurization and methods (re)activating the methane hydrate reservoir.

One elegant way to activate the methane hydrate reservoir is the injection of CO_2. Since CO_2 hydrate is thermodynamically more stable than CH_4-hydrate and both form structure-I, the exchange reaction will proceed exothermically [16], adding heat to the system. Besides its attractiveness in combining energy production with CO_2 storage as a measure to mitigate further increases in greenhouse gas emissions to the atmosphere, a technological advantage is that it sustains the integrity and geomechanical stability of the sediments, thus reducing the potential risk of slope failures.

Several laboratory-based studies have shown the feasibility of the hydrate conversion reaction on pure or sediment-dispersed gas hydrates and from molecular scale to volumes of a few liters (an overview is given in *Discussion*). However, the overall reaction rate turns out to be quite sluggish and the conversion is often incomplete. This results primarily from a shell of CO_2-hydrate that forms around the methane hydrate grain. Any further mass transport of CO_2 into and CH_4 out of the inner core is drastically slowed down or even completely inhibited as analogous experiments with C_2H_6 as attacking guest molecules have shown [17]. Moreover, excess water, as usually encountered in the pore space of hydrate deposits, generally induces immediate CO_2-hydrate formation blocking permeable pathways for the gas exchange.

Common to all those studies is that the chosen pressure-temperature conditions were either within the stability fields of CO_2- and CH_4-hydrate or only CO_2-hydrate. Hence, any attempt towards economic CH_4 production rates based on the CH_4-to-CO_2-hydrate conversion requires a different approach.

In the Ignik Sikumi Gas Hydrate Field Test (January-April 2012) [11] on the Alaska North Slope a 2-stage Huff'n'Puff-like procedure was, thus, followed. First a CO_2/N_2 gas mixture (~6000 m^3 over 13 days) was injected into the CH_4-hydrate bearing sandstone. Subsequently, gas was produced by depressurization for 6 weeks with CH_4 contents dominating the produced gas mixture already after 2 days [18].

Here, we present a different strategy: in our experiments we have injected hot (95 °C), supercritical CO_2 into CH_4-hydrate bearing sand at typical marine *p*-/*T*-conditions. The hot CO_2 was injected in several discrete intervals, actively dissociating the CH_4-hydrate. Each injection was followed by a period of thermal and chemical equilibration of the system. The results are analyzed and presented in terms of CH_4 production rate and overall CH_4 yield, hydrate conversion efficiency, degree of CO_2 and H_2O retention in the system, as well as efficiency of the energy input for CH_4-hydrate dissociation. Partitioning of the components CO_2 and CH_4 into the different liquid, gaseous and hydrate phases is estimated and the results are compared in light of previous experiments which used cold CO_2. Finally, we conclude with perspectives for this hydrate exploitation strategy and outline the steps that are necessary to develop a successive exploitation strategy for marine gas.

2. Experimental Section

2.1. Preparation of Artificial Sediment and Seawater Medium

The sediment samples were prepared at −20 °C from a homogeneous mixture of quartz sand (grain size 0.1–0.6 mm, G20TEAS, Schlingmeier, Schwülper, Germany) and fine grained ice particles (grain size fraction 0.3–1.0 mm, deionized water). Individual sample compositions before and after CH_4-hydrate formation are summarized in Table 1. The sample mixture of quartz sand and ice was filled into a sample bag made of PTFE cloth and was placed inside a stainless steel pressure vessel which was cooled to −7 °C. The pressure vessel was then pressurized with CH_4 gas to 13 MPa. To accelerate hydrate formation, water availability was increased by freezing-thawing cycles from −7 °C to +2 °C in a procedure similar to [19]. The formation process was continuously monitored by logging the CH_4 gas pressure. Within 3–7 days, the conversion of water to hydrate was completed. Subsequently, the sample was brought to −5 °C before being de-pressurized to atmospheric pressure. System re-pressurization and water saturation of pore spaces was achieved by instant filling and re-pressurization with saltwater medium (S ≈ 31). The volumes of saltwater injected into the pressure vessel accounted for the total pore/cavity volumes and are listed in Table 1. Hydrate dissociation during the brief period of depressurization was minimized by taking advantage of the anomalous self-preservation effect, which reaches an optimum close to the chosen temperature [20]. Subsequently, the sample temperature was changed to match the individual requirement of the experiments. Saltwater medium was prepared according to [21] and was close to seawater composition.

Table 1. Sediment preparation and CH_4-hydrate formation. List of initial parameters for sediment and hydrate preparation.

Experiment		Quartz sand/g	Ice/g	Void volume/mL	CH_4-hydrate produced from ice/mol
No.	Experimental conditions				
1	2 °C, 13 MPa	1449	314	1112	3.03
2	8 °C, 13 MPa	1338	297	1172	2.87
3	10 °C, 13 MPa	1514	305	1097	2.95
4	8 °C, 7.5 MPa	1603	315	1053	3.04

2.2. Experimental Setup and Procedure

Experiments were carried out in a custom-made high pressure apparatus (NESSI, Natural Environment Simulator for Sub-seafloor Interactions). All wetted parts of the set-up are made of stainless steel. Saltwater medium was supplied from reservoir bottles (DURAN, Wertheim, Germany) using a HPLC pump S1122 (SYKAM, Fürstenfeldbruck, Germany), CO_2 was supplied with a piston pump (Teledyne ISCO, Lincoln NE, USA) and heated to 95 °C inside a temperature controlled conditioning chamber prior to injection into the sample vessel. Experiments were carried out in upflow mode with injection of CO_2 at the bottom of the sample vessel. Pressure, salinity and temperature were monitored in the influent and the effluent fluid streams. Flow control was achieved by the high-pressure pumps that supplied the fluids. Pressure was adjusted with a back-pressure regulator valve (TESCOM Europe, Selmsdorf, Germany) in line with a fine-regulating valve for compensation of pressure spikes (TESCOM Europe). All experiments were carried out at constant temperature conditions. Temperature control was achieved with a thermostat system (Huber, Offenburg, Germany). The experimental scheme is shown in Figure 1.

Four experiments were carried out at different pressure-temperature (*p*-/*T*-) conditions: 2 °C, 13 MPa; 8 °C, 13 MPa; 10 °C, 13 MPa and 8 °C, 8 MPa. The phase diagram in Figure 2 visualizes the experimental conditions with respect to the thermodynamic stability regimes of CH_4- and CO_2-hydrate.

At the beginning of each CO_2 injection experiment, the water-saturated sediment-hydrate sample was continuously percolated with saltwater medium at a flow rate of 1.0 mL·min^{-1}. This initial water injection interval was performed to verify that the sample body was permeable and homogeneously pressurized. Injection of $CO_{2,sc}$ was realized stepwise, in 4 to 6 injection intervals, simulating a sequential injection strategy as opposed to a continuous injection. During each injection interval, $CO_{2,sc}$ was injected at constant flow rates of 2.5 to 5 mL·min^{-1}.

In between injection intervals, the system pressure was maintained by injection of small amounts of CO_2 at constant pressure. This was necessary to compensate for volume changes due to cooling of the injected CO_2 and to phase changes. The time intervals between injection steps are referred to as equilibration intervals during which no effluent fluid was produced. The number of injection intervals was chosen to ensure at least matching ratios between the injected CO_2 volume and the volume potentially accessible to fluid within the pressure vessel. In most experiments, this was achieved after five injections. However, at 2 °C, 13 MPa, the experiment had to be aborted after the fourth injection due to substantial loss of hydraulic conductivity.

Figure 1. Experimental scheme. (**a**) Experiments were carried out in a high-pressure experimental system suitable for flow-through experimentation. Water and CO_2 were supplied from reservoir containers using suitable high-pressure delivery systems. The hydrate-sediment sample was prepared in a 2 L stainless steel pressure vessel inside an internal pouch made of PTFE cloth. Before entering the pressure vessel, the pressurized CO_2 was heated to 95 °C. The sample-temperature was controlled by circulating cooling fluid through a cooling jacket around the pressure vessel. Pressure, temperature, and conductivity (PTS) were measured discontinuously in the influent and effluent fluids. Bulk effluent fluids were de-pressurized and collected downstream in a 100 L gas sampling bag after de-pressurization; (**b**) Cross-section of the sample pressure vessel.

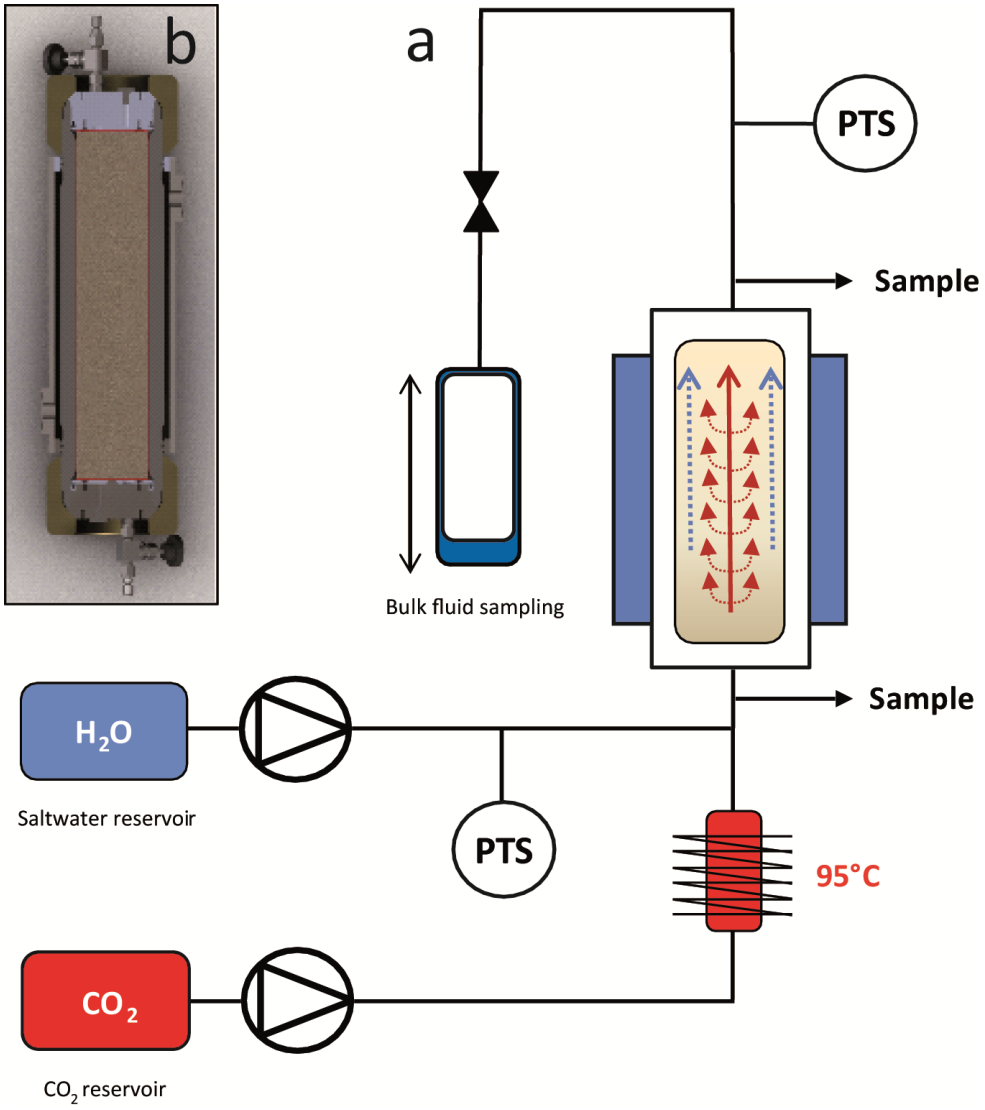

Figure 2. Experimental conditions, stability of CH_4- and CO_2-hydrates. Phase diagrams of the CH_4-H_2O (red) and the CO_2-H_2O (blue) system at S = 31 and pressure-temperature *(p-/T-)* conditions of the respective experiments. Phase diagrams were calculated according to ([22–24]). Experiment 1 was carried out under low-temperature conditions at 2 °C, 13 MPa, inside the stability region of both CH_4-hydrate and CO_2-hydrate. Experiment 2 was carried out at an increased sediment temperature of 8 °C and 13 MPa. Experiment 3 was carried out at 10 °C, 13 MPa inside the stability zone of pure CH_4-hydrate but outside of the stability region of pure CO_2-hydrate. Experiment 4 was carried out at the same temperature conditions as experiment 2 but at a reduced pressure of 8 MPa, close to the phase boundary of pure CH_4-hydrate.

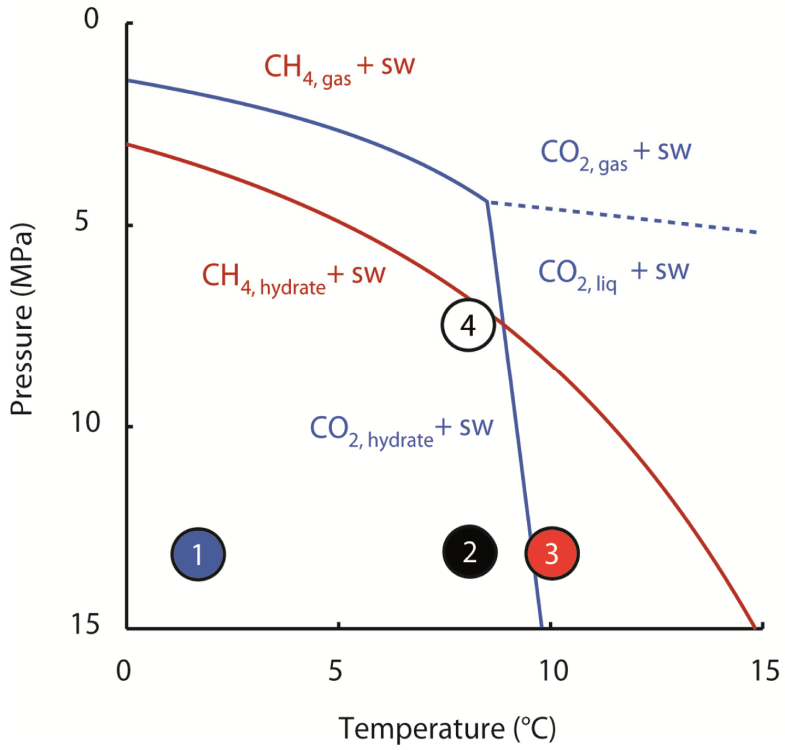

2.3. Fluid Sampling and Gas Analysis

Sub-samples for fluid composition monitoring were taken discontinuously from the influent and effluent streams using gas-tight glass syringes. Gas volumes were measured after expansion at atmospheric pressure. Bulk effluent fluids were collected inside 100 L gas tight TEDLAR sampling bags (CEL Scientific, Santa Fe Springs, CA, USA). The sampling bags were mounted inside water filled sampling containers. After expansion of the effluent fluids at atmospheric pressure, their volume was measured as volume of displaced water from the containers. Effluent gas analysis was carried out with gas chromatography.

2.4. Terms and Definitions

2.4.1. Components and Phases

At the beginning of each experiment, the system consists of three components CH_4, H_2O and quartz sand. All CH_4 is bound in a single phase as CH_4-hydrate ($CH_{4,hyd}$). H_2O is present as liquid salt water or as solid phase hydrate water. The quartz sand is assumed to remain chemically unchanged as an inert solid phase. Injection of supercritical CO_2 ($CO_{2,sc}$) introduces one additional component and three additional phases, CO_2-hydrate ($CO_{2,hyd}$), liquid CO_2 ($CO_{2,liq}$) and gaseous CH_4, ($CH_{4,g}$). Because of mutual solubilities of components, phase composition is somewhat more complicated, which is, however, only of minor importance for this study.

The formation of mixed CO_2-CH_4-hydrates of variable composition in our experiments is likely. However, in this study we were not able to determine the final composition of the gas hydrates at the end of the experiments. Moreover, the exact composition of the gas hydrates does not affect the calculated mass and volume balances and hence the interpretation of our results. Thus, for simplicity reasons, hereafter the term "CO_2-hydrate" is used for gas hydrates containing CO_2, regardless of the fact that they will likely also contain methane in variable amount. Mass flow analysis is exclusively based on component inventories, whereas phase composition is calculated based on volume balancing of influent and effluent fluids.

2.4.2. Calculation of Mass Balances

Mass balances were calculated from measurements of influent (subscript *infl*) and effluent (subscript *efffl*) substance amounts n_{CO2}, n_{CH4}, and masses m_{H2O}. Mass balances are exclusively based on overall amounts of components, but do not consider phase distribution. Experimental results are presented as bulk sample inventories of components *i.e.*, amounts of components inside the pressure vessel. Data evaluation is based on calculation of efficiency (E_{CH4}), yield (Y_{CH4}), and rate (r_{CH4}) of CH_4 production from CH_4-hydrate bearing sediments at different sediment temperatures and pressures, and efficiency (E_{CO2}, E_{H2O}) and amount of CO_2 and H_2O retention (S_{CO2}, S_{H2O}).

The usage of the term efficiency, (E) always relates to the cumulative amount of CO_2 injected ($n_{CO2,inj}$), the subscript *init* refers to the initial amount or mass of component:

$$E_{CH_4} = \frac{Y_{CH_4}}{\sum n_{CO_{2,infl}}} \quad (1)$$

$$E_{CO_2} = \frac{S_{CO_2}}{\sum n_{CO_{2,infl}}} \quad (2)$$

Yield, (Y) refers to the cumulative amount of produced components:

$$Y_{CH_4} = \sum n_{CH_{4,effl}} \quad (3)$$

Retention, (S) is related to the amount of substances that remain in the sample vessel:

$$S_{CO_2} = \sum \left(n_{CO_{2infl}} - n_{CO_{2,effl}} \right) \quad (4)$$

$$S_{H_2O} = \sum \left(m\, H_2O_{init} - m\, H_2O_{effl} \right) \quad (5)$$

We use the term CO_2 retention rather than CO_2 storage to describe the time-dependent accumulation of CO_2 in the sample matrix. This takes into account that on the time scale of the experiments the conversion to CO_2-hydrate is not complete and CO_2 remains partly mobile.

2.4.3. Calculation of Volume Balances

Evidence of phase changes, *i.e.*, dissociation of $CH_{4,hyd}$, with release of $CH_{4,g}$ and formation of $CH_{4,hyd}$ or $CO_{2,hyd}$ was derived from a comparison of the influent and effluent fluid volumes, which were converted to account for the thermodynamic conditions inside the sample vessel (subscript PT).

The release of $CH_{4,g}$ from $CH_{4,hyd}$ is the only process which can account for substantial positive fluid volume differences ($V_{diff,rel}$) with larger bulk effluent fluid volumes compared to influent CO_2 volumes. CH_4 release summarizes the volume of produced CH_4 ($V_{CH4,effl}$) and the volume of $CH_{4,g}$ retained in the pressure vessel according to Equation 6. V_{CO2} and V_{H2O} are symbols for volumes of CO_2 and H_2O:

$$V_{diff,rel} = V_{CO_2,effl,PT} + V_{CH_4,effl,PT} + V_{H_2O,effl} - V_{CO_2,infl,PT} \quad (6)$$

Similarly, negative volume differences ($V_{diff,for}$) in the converted influent and effluent volumes were interpreted as volume consumption of $CO_{2,liq}$ or $CH_{4,g}$ due to hydrate formation. Hydrate formation capacity is calculated based on Equation (7) rather than on Equation (6), which takes into account that CH_4 production from $CH_{4,hyd}$ does not induce a relevant volume difference inside the pressure vessel:

$$V_{diff,\,for} = V_{CO_2,\,effl,\,PT} + V_{H_2O,\,effl} - V_{CO_2,\,infl,\,PT} \quad (7)$$

Volume differences caused by gas dissolution were of minor importance for this study. However, since particularly dissolution of CH_4 in $CO_{2,liq}$ and dissolution of CO_2 in H_2O could become relevant in short term experiments, the maximum error related to our results is estimated in the *Results* section. Quantitative evaluations of CH_4 release and hydrate formation are always in accordance with inventory limits of components.

2.4.4. Calculation of Energy Efficiency

We use a simplified energy ratio to estimate energy efficiency, $E_{\Delta H}$. The energy efficiency relates the theoretical energy input for CH_4-hydrate dissociation to the thermal energy input from injection of hot $CO_{2,sc}$:

$$E_{\Delta H} = \frac{m_{CH_{4,hyd}} \cdot \left(C_{p,CH_4-H} (T_{diss} - T) + \Delta H_{diss} \right)}{m_{CO_{2,infl}} \cdot \left(\Delta H_{f,T,p} - \Delta H_{f,95°C,p} \right)} \cdot 100 \quad (8)$$

We again carefully distinguish between CH_4 production and CH_4 release and calculate energy efficiencies for produced CH_4 ($E_{\Delta H,prod}$, based on mass balance analysis to calculate the mass of hydrate to match produced CH_4) and released CH_4 ($E_{\Delta H,rel}$, based on analysis of fluid volume differences to calculate the mass of hydrate to match released CH_4). The meaning of further symbols in Equation 8 is as follows: $C_{p,CH4\text{-}hyd}$: Specific isobaric heat capacity [25], T_{diss}: dissociation temperature of CH_4-hydrate, T: experimental temperature, ΔH_{diss}: enthalpy of CH_4-hydrate dissociation, $m_{CO2,infl}$: mass of injected CO_2, $\Delta H_{f,T,p}$: enthalpy of formation at experimental pressure and temperature, $\Delta H_{f,95\ °C,p}$: enthalpy of formation at 95 °C and experimental pressure.

3. Results

3.1. Analysis of Mass Balances

3.1.1. CH_4 Inventory and CO_2 Inflow during Injection and Equilibration Periods

Mass balances were calculated from measured compositions of influent and effluent fluid streams. Figure 3 shows the time-dependent CH_4 inventory and the cumulative amount of injected CO_2 during the whole experimental period. The bulk sample composition was altered considerably by production of CH_4 and retention of CO_2 during injection/production intervals, but was only slightly changed during equilibration intervals as a result of pressure-controlled slow injection of CO_2.

CH_4 production was clearly dependent on sediment temperature and hydrostatic pressure. Between 2% and 35% of the initial amount of CH_4 fixed in hydrate was produced after stepwise injection of 22 mol and 21 mol CO_2 (Figure 3a at 2 °C, 13 MPa and 3d at 8 °C, 8 MPa, respectively). From the graphs of effluent fluid pressure in Figure 3, it is apparent that pressure is not constant during injection periods. Pressure oscillations are partly due to the backpressure regulation mechanism where pressure is discontinuously released by a valve, or due to accidental freezing of regulators after cooling from adiabatic gas expansion. However, exceptionally large pressure spikes were observed in Experiment 1 at 2 °C, 13 MPa. These pressure spikes occurred after sample permeability decreased drastically, suggesting rapid CO_2-hydrate formation. Permeability could only be restored after sample fracturing with very high differential pressures >15 MPa. Sample blocking became irreversible by experimental means at the end of Experiment 1.

Figure 3. Inventory of CH_4, cumulative amount of injected CO_2 and sample effluent pressure (p_{effl}) in each of the experimental runs. (**a**) 2 °C, 13 MPa; (**b**) 8 °C, 13 MPa; (**c**) 10 °C, 13 MPa; (**d**) 8 °C, 8 MPa. It should be noted, that the axis scaling for p_{effl} is different for every experiment. CO_2 was injected stepwise as hot supercritical $CO_{2,sc}$ and at a constant flow rate (steep gradients in dashed lines). Injection of CO_2 at constant pressure and low flow rate alternated with equilibration periods. Fluids including CH_4 could only exit the system during injection/production periods. CH_4 production is shown as a decrease of the CH_4 inventory. Effluent fluid pressure (p_{effl}) is constant during equilibration periods. Strong aberrations indicate technical problems, which could be solved without destabilization of the hydrate sample. However, p_{effl} is unstable during injection periods. Massive pressure spikes were observed in Experiment 1 (2 °C, 13 MPa) after sample permeability changed due to CO_2-hydrate formation. Sample permeability could be restored temporarily by fracturing at high differential pressures (>15 MPa). CO_2-hydrate formation eventually led to complete congestion of the fluid pathways at the end of the experiment. Sample blocking was not observed in other experiments at higher temperatures.

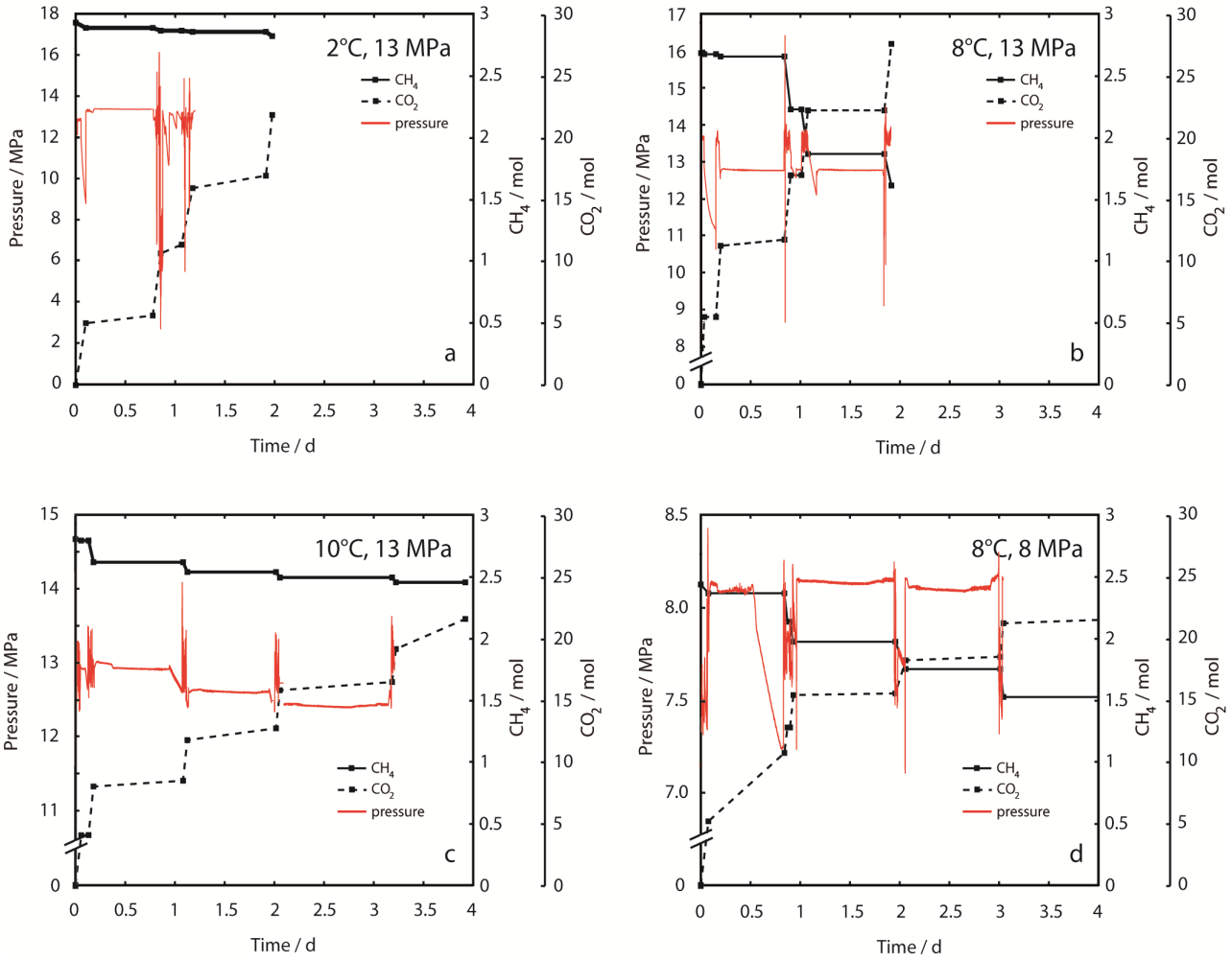

3.1.2. CH_4 Production

Generally, data in this study are presented as amounts of substance or masses of the components CH_4, CO_2 and H_2O which were retained inside the pressure vessel, *i.e.*, the development of the inventory of the respective components in the bulk sample, as a function of the amount of injected CO_2. This approach allows for easy comparison of CH_4 production efficiencies as shown in Figure 4. Changes in inventory amounts are calculated by balancing substance amounts of influent and effluent fluids. Results in Table 2 indicate that CH_4 concentration in the overall effluent gas was comparatively high during early injection steps. However, only small amounts of bulk effluent gas consisting of both CH_4 and CO_2 were produced. During later injection steps, the produced fluid volume is much larger with high amounts of CO_2 contributing to the effluent gas. Therefore, the absolute amounts of produced CH_4 are increased while the relative amounts of CH_4 are decreased. We found that CH_4 production from CO_2 injection is most efficient at 8 °C, while the gas recovery was apparently independent of pressure. CH_4 recovery at 2 °C and 10 °C was both impaired compared to experiments at 8 °C. The experiment at 8 °C, 13 MPa was terminated after the injection of 27.5 moles of CO_2. At this point, 31% of the available hydrate reservoir was depleted and produced as effluent CH_4. Particularly at 8 °C, CH_4 production showed a linear trend with respect to CO_2 injection, which indicates that CH_4 from the CH_4 inventory can be produced with constant efficiency using $CO_{2,sc}$. The experiments were stopped before reaching a maximum production yield after the volume of injected CO_2 was approximately equal to the sample void volume.

Figure 4. CH_4 production. CH_4 sample inventory during injection of CO_2. Low CH_4 production efficiency and yield was observed at 2 °C, 13 MPa (▲) and 10 °C, 13 MPa (♦). CH_4 production efficiency and yield were highest at 8 °C (both runs).

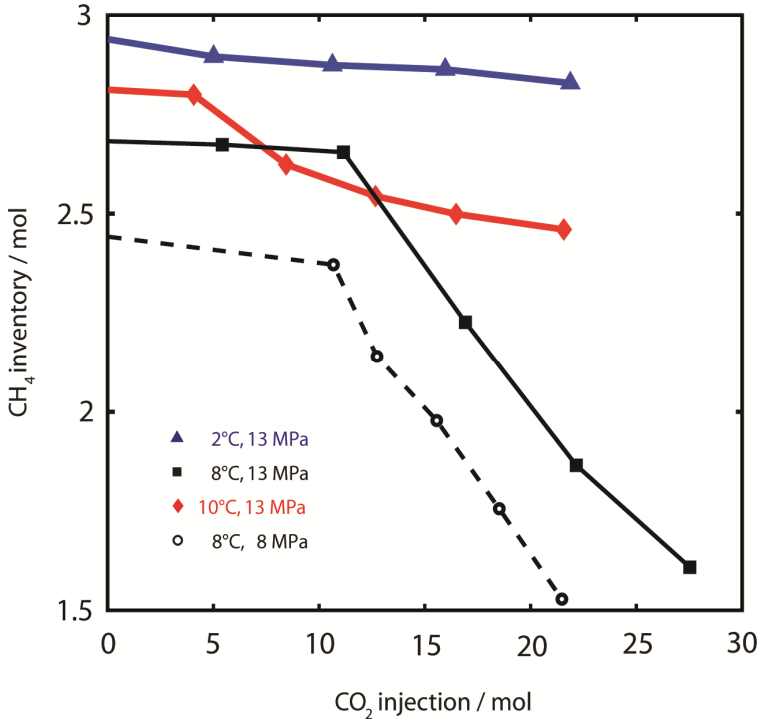

During the initial saltwater percolation period prior to CO_2 injection (data not shown), only minor amounts of CH_4 were produced with the effluent water. The continuously injected saltwater is undersaturated with respect to CH_4 and therefore stimulates the dissociation of CH_4-hydrates until saturation is reached. The occurrence of this effect indicates a satisfactory surface contact between the percolating liquids and the hydrate. However, the production of free $CH_{4,g}$ was not observed during the saltwater percolation period.

Table 2. Effluent amounts of CH_4 and CO_2. Amounts of CH_4 and CO_2 recovered in the effluent fluid for each injection step. The third column for each injection step shows the CH_4 content in the effluent gas consisting of only CH_4 and CO_2. Although the amounts of effluent CH_4 increase, the CH_4 content is low because of large amounts of effluent CO_2

Experimental Conditions	Effluent gas composition														
	Inj. Step 1			Inj. Step 2			Inj. Step 3			Inj. Step 4			Inj. Step 5		
	n (mol)		CH_4 /% (v/v)	n (mol)		CH_4 /% (v/v)	n (mol)		CH_4 /% (v/v)	n (mol)		CH_4 /% (v/v)	n (mol)		CH_4 /% (v/v)
	CH_4	CO_2		CH_4	CO_2		CH_4	CO_2		CH_4	CO_2		CH_4	CO_2	
2 °C, 13 MPa	0.004	0.02	**17.3**	0.022	1.16	**1.8**	0.011	1.44	**0.7**	0.034	2.21	**1.5**	/	/	/
8 °C, 13 MPa	0.009	0.02	**29.3**	0.019	0.01	**65.2**	0.317	3.33	**8.7**	0.237	4.09	**5.5**	0.255	4.05	**5.9**
10 °C, 13 MPa	0.142	1.45	**8.9**	0.175	2.81	**5.9**	0.079	2.71	**2.8**	0.044	2.86	**1.5**	0.039	2.55	**1.5**
8 °C, 8 MPa	0.070	0.05	**56.2**	0.231	1.50	**13.3**	0.162	2.3	**6.5**	0.221	2.4	**8.4**	0.227	2.7	**7.7**

3.1.3. CO_2 and H_2O Retention

In addition to CH_4 production, the efficient retention of CO_2 and H_2O is important for the overall process. As shown in Figure 5, CO_2 retention was most efficient at 2 °C, 13 MPa, where the thermodynamic conditions were most favorable for CO_2-hydrate formation. Increasing amounts of CO_2 were retained over the entire experimental period with a linear increase in the CO_2 inventory until the experiment was stopped after loss of hydraulic conductivity. Also in experiments at higher temperatures the maximum CO_2 retention capacity was not reached until the end of the experiments. However, CO_2 retention efficiency was lower than at 2 °C. Similar to CH_4 production, differences in CO_2 retention were minor in experiments at 8 °C at different pressures. While the retention during the first injection steps was comparable to the retention at 2 °C, it was less efficient during later injection steps ($n_{CO_2,inj}$ > 10 mol) where substantial amounts of the injected CO_2 were produced in the effluent gas stream. At 10 °C, 13 MPa, *i.e.*, slightly above the CO_2-hydrate dissociation temperature, CO_2 breakthrough occurred almost immediately after injection.

In contrast to CH_4 production and CO_2 retention, the efficiency of water retention was similar in all experiments. Approximately 50% of the initial water was retained in the pressure vessel at all temperatures and pressures (Figure 6).

Figure 5. CO_2-retention. CO_2 sample inventory during injection of CO_2. CO_2 retention efficiency was highest at 2 °C, 13 MPa (▲). Rapid CO_2 breakthrough was observed at 10 °C, 13 MPa (♦). CO_2 retention efficiency at 8 °C (■, 13 MPa and ○, 8 MPa) was dependent on pressure conditions.

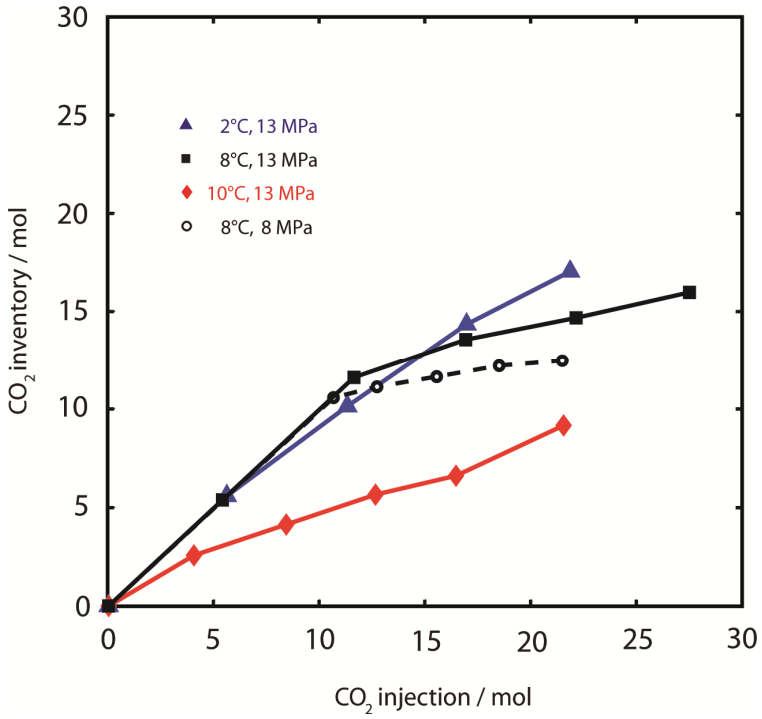

Figure 6. Water retention. H_2O sample inventory during injection of CO_2. Retention of pore water was similar for all experiments with approximately 50% of initial water content (pore water plus hydrate water) being removed.

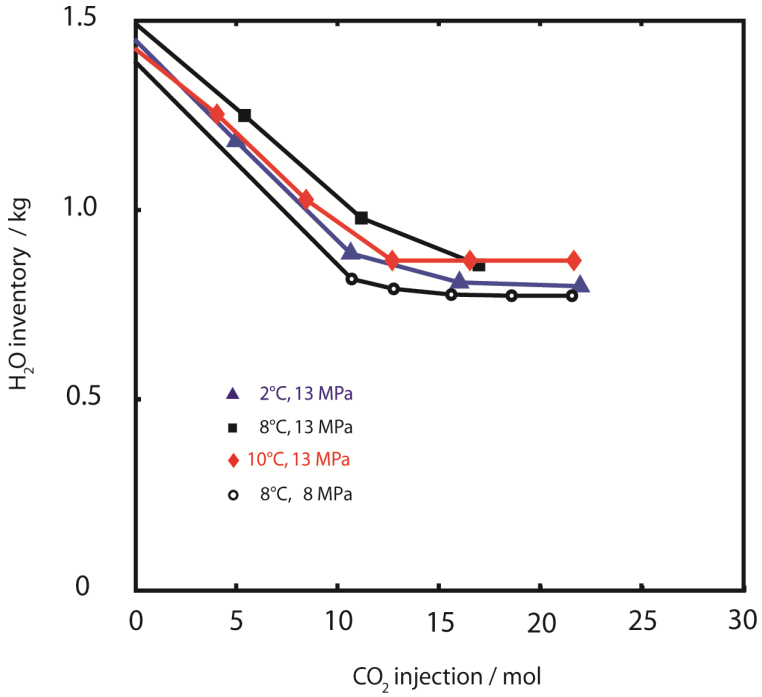

Typical conductivity values from discontinuous measurements of bulk effluent water samples were 10.3 ± 3.5% below influent saltwater conductivities, indicating partial freshening of the pore water by hydrate water. A small number of samples showed exceptionally low conductivity values compared to influent saltwater medium values (injection step 2 at 10 °C, 13 MPa: 16% of saltwater conductivity, injection step 4 at 8 °C, 8 MPa: 67% of saltwater conductivity). These substantial differences could be due to errors during sampling. However, in accordance to volume balance calculations in the next paragraph they are probably due to distinct events of discharge of low salinity hydrate water released from hydrate dissociation. Conductivity measurements were not used to quantify hydrate dissociation inside the reactor since it was not possible to adequately calculate effects of mixing and transport of H_2O in the pressure reactor. Additionally, amounts of discharged H_2O were relatively small and could be easily contaminated by leakage of water from the sampling container into the sampling bag. Because of such a leak in the sampling bag, water inventory values for the two last injection steps at 8 °C, 13 MPa could not be calculated.

3.1.4. Investigation of Sampling and Analytical Error

Error in results was investigated from mass balancing after release of fluids from the high-pressure vessel at the end of Experiments 3 and 4. However, mass balance analysis was not carried out in Experiments 1 and 2, since we have attempted to sample undisturbed hydrates at the end of each experiment instead. While fluid release for mass balancing had to be performed slowly, hydrate sampling has to be performed fast and demanded rapid release of remaining pressurized fluids.

However, depressurization and bulk effluent sampling after completion of the experiment by stepwise releasing large amounts of $CO_{2,liq}$ via the manually adjusted backpressure regulator was very problematic. The instant expansion of the CO_2, especially after lowering the backpressure, led to pressure spikes in the sampling lines and bag due to flow restrictions in the tubing which had a length of several meters. This caused substantial leakage and extensive loss of effluent gas, which could be visually observed. Pressure spikes were even more distinct and severe due to frequent freezing of the valves from adiabatic gas expansion and subsequent expulsion of CO_2 after required additional lowering of the backpressure settings and warming of the frozen valve and tubing. However, this effluent gas loss during final depressurization was of minor importance during the experiment because of much lower flow rates and no adjustment of the backpressure regulator being necessary.

Because of these problems with depressurization, final recovery of CO_2 and CH_4 showed some deviation with respect to amounts of injected CO_2 or initial CH_4 amounts. The error in CO_2 recovery was −6.5 mol CO_2 (30% from total injected CO_2) in experiment 3, and −3.4 mol CO_2 (16% from total injected CO_2, in experiment 4). Mass balance deviations for CH_4 were −1.2 mol (40% from initial CH_4) in experiment 3 and 0.4 mol (14% from initial CH_4) in experiment 4. However, water recovery was excellent in both experiments with a cumulative relative error of < 2%.

3.2. Analysis of Volume Balances

While mass balances allow for the calculation of the quantities of different components inside the sample vessel, they do not provide any information on the distribution of the components among the liquid, gas and hydrate phases. Influent and effluent fluid volumes corrected to experimental pressure

and temperature were analyzed as a measure to further constrain the amounts of $CH_{4,g}$ and to evaluate the reservoir size of CH_4- and CO_2-hydrate. Effluent volumes include the cumulative amounts of CH_4, CO_2 and H_2O in the production fluid; the influent volume is exclusively composed of injected CO_2.

CH_4 released in Figure 7 summarizes the amount of CH_4 produced (red areas) and $CH_{4,g}$ retained in the pressure vessel (pink areas) after hydrate dissociation. Release of CH_4 from dissociating hydrates causes $V_{diff,rel}$ to positively deviate from the neutral volume balance in Figure 7. However, $V_{diff,for}$ used for estimating hydrate formation (shown as blue areas in Figure 7), does not consider CH_4 production in the volume balance, thus both hydrate formation and $CH_{4,g}$ accumulation are shown as simultaneous events in Figure 7. The exclusion of $CH_{4,effl}$ from the volume balance is motivated from considering that CH_4-hydrate dissociation releases $CH_{4,g}$ and H_2O. Thus, CH_4 production from hydrates does not induce a relevant volume difference inside the pressure vessel. In contrast, CH_4 production from $CH_{4,g}$ induces a volume difference, and hydrate formation capacity estimated from fluid volume balancing would be lowered accordingly. Since it is currently not possible to distinguish between the possible sources of produced CH_4, we assume that all produced CH_4 originates from hydrate dissociation.

Figure 7. Fluid volume balancing and evaluation of phase distribution. Deviations from even volume balances [grey dashed lines in (**a**)–(**d**)] are shown as colored areas related to the cumulative volume of injected CO_2. The figure emphasizes the difference between CH_4 production (red areas) and CH_4 release (pink areas plus red areas). The volume based hydrate formation potential was derived from negative volume differences (blue areas). Results are presented for single experiments (**a**) 2 °C, 13 MPa; (**b**) 8 °C, 13 MPa; (**c**) 10 °C, 13 MPa; (**d**) 8 °C, 8 MPa. Volume balances were calculated from inflow amounts of CO_2 and effluent amounts of CO_2, CH_4 and H_2O for each injection step. During early injection steps most positive deviations were observed with largest net deviations for 10 °C, 13 MPa (**c**). Distinct negative deviations were observed in the experiments at 2 °C and 10 °C during later injection steps. Positive deviations are considered to be entirely due to CH_4 gas release from CH_4-hydrates, whereas negative deviations are considered to be due to hydrate formation of either CO_2-, CH_4- or mixed CO_2-CH_4-hydrates.

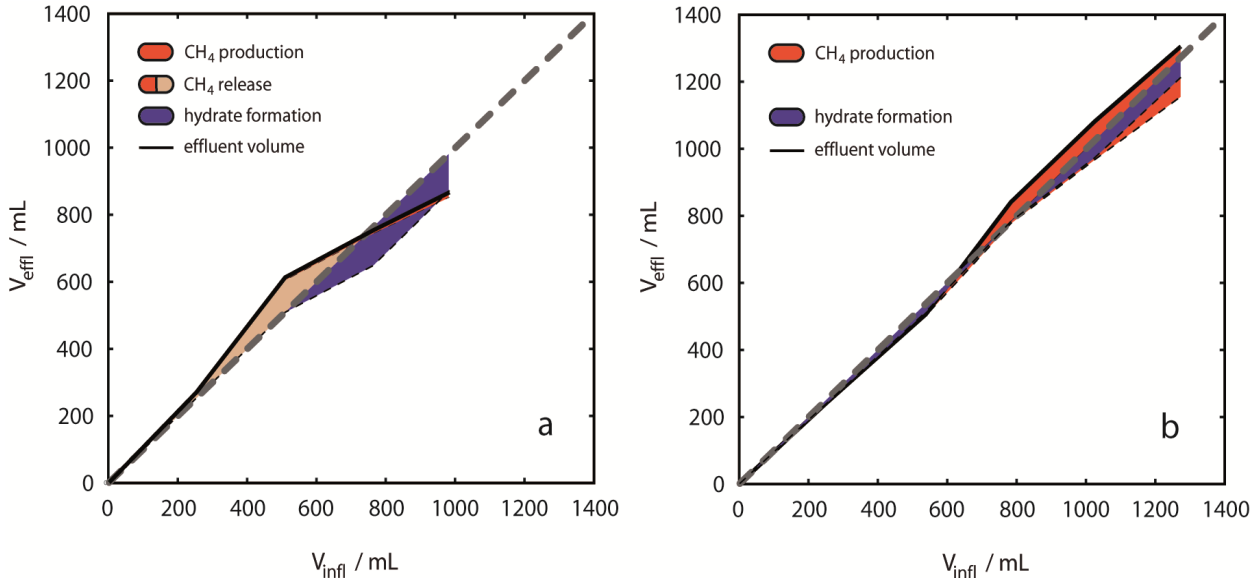

Figure 7. *Cont.*

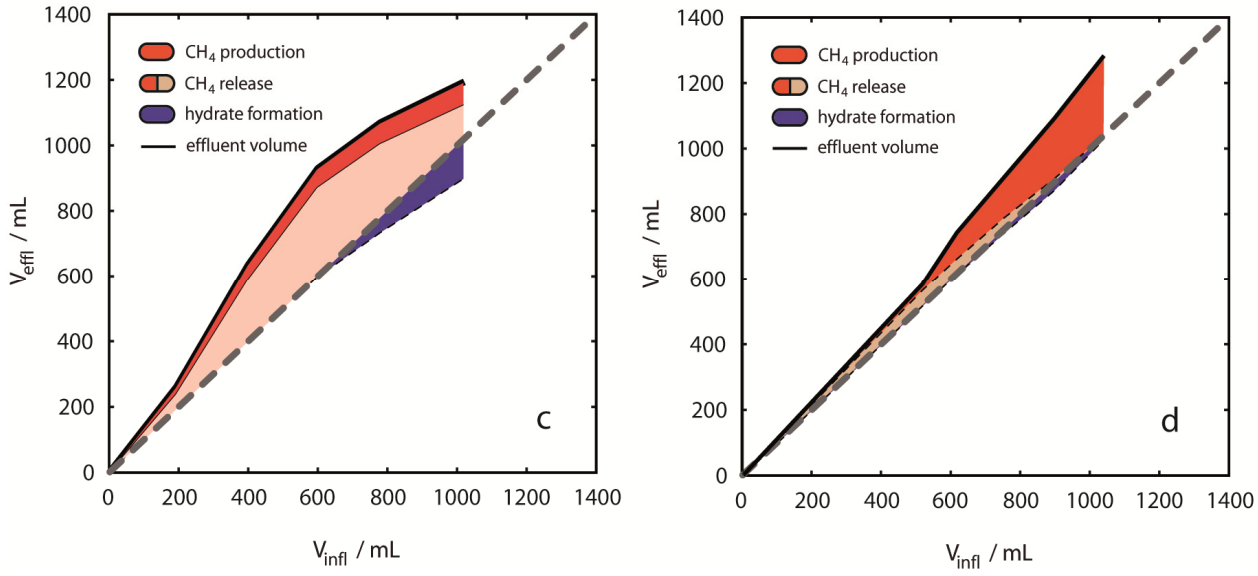

Overall $V_{diff,rel}$ revealed different tendencies with respect to *p*-/*T*-conditions. Only in Experiment 1 at 2 °C, 13 MPa overall $V_{diff,rel}$ was negative (−115 mL, 12% of volume of injected CO_2). All other experiments revealed positive volume differences. At 8 °C, 8 MPa $V_{diff,rel}$ was +246 mL (24% of volume of injected CO_2) and at 10 °C, 13 MPa $V_{diff,rel}$ was +182 mL (18% of volume of injected CO_2). In contrast, the overall fluid volume balance of +31 mL (3% of volume of injected CO_2) was small, but still positive at 8 °C, 13 MPa. Experiments at 2 °C and 10 °C showed a trend to positive volume change values during early injection steps, whereas negative values were observed mainly during the late injection steps. Such a trend was not observed in the experiments at 8 °C. CH_4 release was clearly exceeding CH_4 production in experiment 3, but also in Experiment 1, volume differences indicated transient CH_4 release without CH_4 production. The smallest apparent differences between volumes of produced CH_4 and released CH_4 are observed in experiments at 8 °C.

Volume differences caused by component dissolution were neglected here, however, in all cases of dissolution of a pure component an error is introduced in the volume analysis. Particularly dissolution of CH_4 in $CO_{2,liq}$ and dissolution of CO_2 in H_2O could be significant. The saturation concentration of CO_2 in an aqueous solution at 10 °C and 13 MPa is approximately 1.6 mol/kg. Dissolution of 1.6 mol of CO_2 of $\rho \approx 942$ kg/m^3 in 1 kg of saltwater $\rho \approx 1030$ kg/m^3 produces a brine of $\rho \approx 1046$ kg/m^3. The volume difference between the resulting brine and the initial two phase liquids amounts to approximately −23 mL that are not accounted for in the volume balance calculations. Only few data are available for estimating the solubility of CH_4 in $CO_{2,liq}$ and the possible error from this phase transfer cannot easily be quantified. Further, the solubility of H_2O in CO_2 and CH_4 phases is of minor importance for volume balancing. However, please note that all phase transfers resulting from mutual solubilities of components would induce a negative volume difference and would finally result in an underestimation of CH_4 release. CH_4 release estimates in this study are therefore minimum values.

3.3. Analysis of Energy Efficiencies

Energy balancing evaluates the efficiency of thermal stimulation of hydrate dissociation. It complements the results from mass and volume balances carried out in the previous paragraphs. We use a simplified energy ratio Equation 8 to estimate energy efficiency of CH_4 production $E_{\Delta H,prod}$ and CH_4 release $E_{\Delta H,rel}$.

Figure 8. Energy efficiency. (**a**) Cumulative energy efficiency of gas production ($E_{\Delta H,prod}$) was calculated from free enthalpy changes comparing effluent CH_4 gas recovery with theoretical CH_4 release from hydrate dissociation due to injection of supercritical CO_2. Lowest $E_{\Delta H,prod}$ was observed at 2 °C, 13 MPa (▲). $E_{\Delta H,prod}$ at 10 °C, 13 MPa (♦) peaked at 11.3%, but decreased with ongoing CO_2 injection. $E_{\Delta H,prod}$ was highest at 8 °C, independent of hydrostatic pressure. The energy efficiency calculated from CH_4 production is compared to the energy efficiency calculated from CH_4 gas release ($E_{\Delta H,rel}$); **(b,** please note the difference in axis scales**)**. Minor differences were observed in experiments at temperatures 8 °C. However, $E_{\Delta H,rel}$ at 10 °C is close to optimum (♦ in (**b**)), whereas energy efficiency of CH_4 production is only 11.3% (♦ in (**a**)). Also at 2 °C, $E_{\Delta H,rel}$ is considerably increased compared to $E_{\Delta H,prod}$. These results indicate that a significant amount of $CH_{4,g}$ liberated from dissociating CH_4-hydrates is trapped and might eventually re-crystallize in secondary CH_4- or (CH_4-CO_2)-hydrates within the sediment.

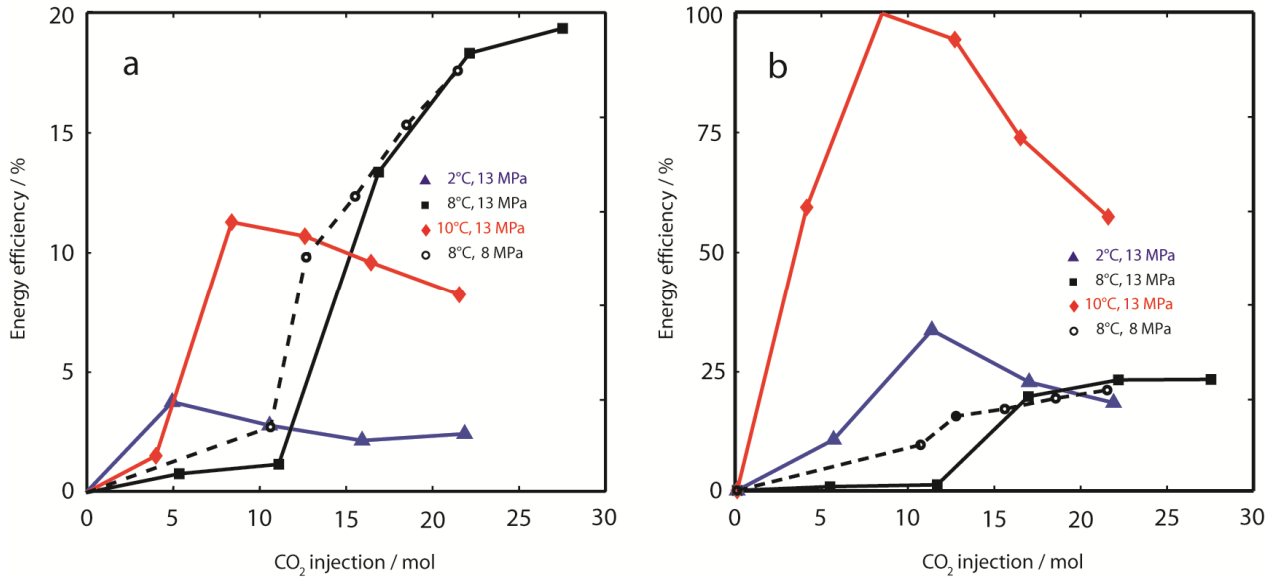

The importance to distinguish between CH_4 production and CH_4 release becomes obvious from Figure 8. Figure 8a shows the cumulative $E_{\Delta H,prod}$ based on CH_4 production yields. While experiments at 8 °C show reasonable energy efficiencies (19% at 13 MPa, and 18% at 8 MPa), energy recovery was apparently poor at 2 °C, 13 MPa (2%) and 10 °C, 13 MPa (8%). In contrast, cumulative $E_{\Delta H,rel}$ based on apparent CH_4 release estimated from fluid volume differences was considerably higher, with maximum efficiency values close to 100% for early injection steps at 10 °C. Although the energy efficiency of CH_4 release due to CO_2-injection was close to optimum values for the highest sediment temperature (10 °C), this was not reflected in CH_4 production, which was relatively inefficient

compared to experiments at lower temperatures. A similar trend was also observed in Experiment 1 at 2 °C, however, $E_{\Delta H,rel}$ was considerably lower compared to the experiment at 10 °C. The increase in cumulative energy efficiency $E_{\Delta H,rel}$ between injection steps 1 and 2 at 10 °C can be explained by a very short equilibration time (0.07 d), which was too short for thermal equilibration of the sample.

4. Discussion

4.1. Effect of Reservoir Temperature

Experiments were conducted at three different reactor temperatures (2, 8 and 10 °C) reflecting typical gas hydrate reservoir temperatures found in the natural environment. As anticipated, at 2 °C CO_2-hydrates formed with the excess pore water rapidly reducing the permeability of the sand matrix and thus, blocking available flow pathways. Applying higher differential pressure enabled fracturing of the sample and renewing fluid flow conditions for a few times, as observed by the high pressure spikes in Figure 3. However, after the fourth injection of CO_2, the experiment had to be aborted as further fracturing of the sample was not possible anymore because the maximum pressure limit of NESSI was reached. This may also illustrate the potential risk of clogging up the surrounding of any CO_2 injection well during CH_4-hydrate production operation under similar unfavorable environmental *p-/T*-conditions.

However, the observations made at higher reactor temperatures, particularly that CH_4 recovery at 8 °C was more efficient than at 10 °C, were unexpected. At an operating pressure of 13 MPa CO_2-hydrate may form at 8 °C, whereas liquid CO_2 and saltwater are the stable phases at 10 °C (Figure 2). Accordingly, the experimental result at 8 °C suggests that formation of CO_2-hydrate in the pore space at comparably moderate rates reduces the permeability locally, thereby diverging the fluid flow to new pathways through the sample. Hence, new regions of the sediment are accessed by the injected CO_2 and new CH_4-hydrates made available for dissociation and CH_4 release. Overall, this leads to a quite evenly distributed migration of the injected CO_2 through the quartz sand and an efficient production of hydrate-bound CH_4.

In contrast, at a reactor temperature of 10 °C the efficiency of the CH_4 gas recovery was much lower, because CO_2-hydrate could not form. As a consequence, permeability increased locally where the injected CO_2 dissociated the CH_4-hydrate, opening up a preferential flow pathway for the injected CO_2. Hence, the injected CO_2 did only affect a small region of the hydrate-bearing sediment and further CH_4-hydrate dissociation is controlled by lateral heat propagation away from the conduit and the respective CH_4 production is in addition also limited by its mass transport towards the channel.

The unexpected similarity of CH_4 production at 8 °C and 8 MPa or 13 MPa (Figure 4) indicated that sediment depressurization only had a minor effect on CH_4 production. However, depressurization and enhanced destabilization of initial CH_4-hydrate in the presence of CO_2 likely resulted in a CO_2-CH_4 gas mixture which could readily induce formation of mixed CO_2-CH_4-hydrates of modified stability relative to pure CO_2- or CH_4-hydrates [26]. Indeed, evidence for re-formation of hydrates with high CH_4 content was found from volume balancing (4.3).

4.2. Supercritical CO_2 as Injection Fluid

The injection of $CO_{2,sc}$ for production of CH_4 from CH_4-hydrates was tested experimentally for the first time. The technical strategy of CH_4 production from hydrates by injection of $CO_{2,sc}$ into the host sediment can be considered as a combination of using an injection fluid for chemical activation of the reservoir with additional thermal stimulation. As a result from this combination CH_4 production from hydrates is accelerated initially since CH_4 release is driven rather by thermal stimulation of hydrate dissociation, than by hydrate conversion. The dominance of heat induced hydrate dissociation over hydrate conversion can be clearly seen from constant CH_4 production efficiencies and the absence of apparent mass transfer limitations which would be expected in a diffusion-controlled conversion mechanism. However, the relevance of thermal hydrate dissociation as compared to hydrate conversion after thermal equilibration of the injected CO_2 with the reservoir needs to be studied in more detail. The relative contribution of thermal dissociation and mass transport controlled hydrate conversion will strongly influence the development of the injection strategy with regard to lengths of injection and equilibration periods.

As we have further shown in this study, heat injection and transport are crucial not only to CH_4-hydrate destabilization but also to flow assurance in the hydrate-sediment porous medium. While different heat injection strategies are potentially feasible, the injection of hot $CO_{2,sc}$ appears to offer some benefits over cold injection of CO_2 combined with independent heat injection strategies, because the combined fluid and heat flow prevents uncontrolled CO_2-hydrate formation in the best possible way.

Calculations of energy efficiency of CH_4 production resulting from injection of hot $CO_{2,sc}$ seemingly indicated substantial heat loss to secondary processes, which has raised questions towards the energetic feasibility of $CO_{2,sc}$ injection. However, this production focused energy balance is somewhat misleading, since CH_4 release is apparently exceeding CH_4 production drastically. In that case, $CH_{4,g}$ mobilization is the actual problem limiting CH_4 production, rather than energy efficiency. This aspect will be discussed in detail in the following paragraph.

While the primary effect of injection fluid temperature *i.e.*, the direct influence on CO_2-hydrate formation, CH_4-release and production is not clear at the moment, this study provides strong evidence that the secondary effect of injection fluid temperature, which is increasing sediment temperature, is very important. Heat transport and sediment warming as a result of injection of $CO_{2,sc}$ was not evaluated in this study. To stronger emphasize the relevance of this secondary effect of injection fluid temperature and also to better reflect reservoir conditions the experimental setup and procedure needs to be adapted to provide a spatially and temporally resolved temperature profile of the sample.

Although the combination with additional process techniques such as depressurization is promising, the CO_2 injection strategy itself is a central engineering tool for process optimization, and further modifications to the injection fluid might be of interest. An unsolved problem is the early breakthrough of CO_2 as observed in our experiments which results in a dilute CH_4 production fluid. The subsequent processing of the production fluid would be technically and economically demanding. As a further aspect, $CH_{4,g}$ mobilization after hydrate dissociation, could potentially be improved by influencing the physical or chemical properties of the injection fluid.

4.3. CH_4 Production and Release

This study clearly reveals the importance to differentiate between CH_4 production and CH_4 release. Mass balance analyses indicated that using the tested injection scheme both CH_4 production and CO_2 retention are best at 8 °C. However, the recovered CH_4 gas only is a fraction of the CH_4 gas being released due to CH_4-hydrate dissociation. That this is true to various extents in the different experiments was concluded from fluid volume balancing, *i.e.*, analysis of fluid volume differences. A positive $V_{diff,rel}$ as calculated by Equation 6 is assumed to be due to dissociation of CH_4-hydrate and release of free gas. In contrast, a negative $V_{diff,for}$ must be due to formation of CH_4-, CO_2- and mixed CH_4-CO_2-hydrate.

We observed strong differences with respect to fluid volume balances in the different experiments. In the experiment at 2 °C, 13 MPa, indicated by marked negative volume differences during later injection steps, a strong tendency towards hydrate formation was observed. This is clearly in accordance with results from mass flow analysis as well as with experimental observations showing the fatal loss of sample hydraulic conductivity. However, negative volume differences were preceded by positive net volume changes which indicated at substantial release of $CH_{4,g}$ from hydrate dissociation. Since only minor CH_4 production was measured in the experiment at 2 °C, $CH_{4,g}$ must have been retained inside the pressure vessel. Hydrate formation in this experiment was hence probably fueled from two reservoirs, $CH_{4,g}$ and $CO_{2,liq}$. The substantial retention of injected CO_2 at 2 °C, $CO_{2,liq}$ suggests that CO_2-hydrate is dominantly formed, however, the formation of mixed CO_2-CH_4-hydrates as well as the re-formation of CH_4-hydrates cannot be excluded.

In contrast to the experiment at 2 °C, fluid volume differences in the experiment at 10 °C were clearly dominated by CH_4-hydrate dissociation and release of $CH_{4,g}$, particularly in the early phase of the experiment. The high efficiency of CH_4 release with respect to thermal stimulation by $CO_{2,sc}$ was clearly shown from energy efficiency calculations. However, the efficiency of CH_4, release was not reflected in CH_4 production and up to 2.1 mol $CH_{4,g}$ which was released from hydrates during CO_2 injection apparently remained as immobile gas inside the sample pressure vessel. The fact that significant amounts of CH_4 remain within the sediment sample raises the question if and to what extent CH_4 recovery is limited by gas mobilization rather than by the release of CH_4 from hydrate. This is an aspect which needs to be investigated carefully in further studies since it influences process optimization strategies drastically. Similar to experiment 1 at 2 °C, volume differences at 10 °C reveal a transition towards hydrate formation during later injection steps. Since pure CO_2-hydrates are thermodynamically not stable under these conditions only the re-formation of CH_4-hydrate or the formation of mixed CH_4-CO_2-hydrates could account for these volume differences. The retention of $CH_{4,g}$ followed by drastic re-formation of CH_4-hydrates is thus the reason for poor CH_4 production efficiencies at 10 °C.

Interestingly, the strong deviations between CH_4 production and CH_4 release were not observed in experiments at 8 °C. It is possible, that under these conditions CH_4-hydrate dissociation and $CH_{4,g}$ release are well balanced by CO_2-hydrate formation and volume differences induced by the simultaneous processes are hidden. The absence of net fluid volume changes could indicate the simultaneous absence of excess CH_4 release and CO_2-hydrate formation as well as substantial excess CH_4 release balanced by CO_2-hydrate formation. Indeed, for all experiments, hydrate formation is

assumed to be a continuous process and not, as suggested from volume balances, only occurring during later injection periods. Of course, if that is true, ongoing hydrate formation would need to be compensated by additional $CH_{4,g}$ release and would further increase the discrepancy between CH_4 production and CH_4 release. It shall be emphasized that fluid volume balancing as carried out in this study only helps to distinguish between dominant processes of CH_4 release or hydrate formation as ratios, and as such, phase inventory values are not readily accessible.

The reason for discrepancies between CH_4 production and apparent CH_4 release are not clear yet. Interestingly, we observed similar trends for the experiment at 2 °C, which is putatively dominated by substantial CO_2-hydrate formation and the experiment at 10 °C, which excludes the formation of pure CO_2-hydrate. It appears possible, that both the fast passage of the CO_2 as observed at 10 °C hinders the efficient CH_4 production as well as slow passage at 2 °C in low permeability sediments dominated by rapid hydrate formation. At 10 °C, injected and rapidly flowing $CO_{2,sc}$ cools via heat conduction and distant melting of CH_4-hydrates, thus producing inaccessible $CH_{4,g}$ inclusions. At 2 °C this effect is possibly modulated and amplified by additional flow restrictions from CO_2-hydrate formation which could shield $CH_{4,g}$ inclusions effectively.

4.4. Comparison of Hydrate Conversion Experiments

In our experiments injection times and subsequent equilibration periods were arbitrarily chosen and varied for several technical and practical reasons within and between experiment runs (Figure 3). The primary goal of our study was to prove the feasibility of our supercritical CO_2 technique under representative *p-/T-* conditions, but it was not intended to optimize its performance and efficiency—this must be left for future work. Therefore, calculating rates of hydrate conversion or methane production will give somewhat arbitrary numbers. However, since these are the first hydrate conversion experiments using supercritical CO_2, it seems necessary and appropriate to compare our results to those of previous studies from other groups where CH_4-hydrates were exposed to cold liquid or gaseous CO_2 (see Table 3).

In our experiments the highest CH_4 yields were achieved at 8 ºC, where 31%–36% of the hydrate-bound CH_4 was produced (Table 3) before those two experiments were, deliberately, aborted after 44 h and 73 h, respectively. At this point a relatively constant methane production had been established (Figures 3 and 4). In contrast, the 10 ºC experiment achieved only a methane yield of 12.5% and shows a considerable decrease in CH_4 production after the second injection cycle. At 2 °C, the methane is quite constantly produced (Figures 3 and 4), but with very low overall yield of only 2.4%.

Table 3. Hydrate conversion experiments.

CO_2 phase	CH_4 yield (%)	Time (h)	Volume (mL)	Sediment	Pressure (MPa)	Temperature (°C)	Hydrate stability	Reactor type	Reference
gas	100	4	90	no	3.5	3	CO_2	batch	[27]
gas	27	280	130	no	3.25	0/(−2/+2)	$CH_4 + CO_2$	batch + flow − through	[28–30]
gas (N_2/CO_2)	85	20	no info	no	12	1	$CH_4 + CO_2$	batch	[31]
gas	100	150	laser spot	no	3.0	5	CO_2	batch	[32]
gas	3	120	420	no	3.3	−2/0/+2	$CH_4 + CO_2$	batch	[33]
liquid	15	700	3200	no	3.9–4.5	1–3	$CH_4 + CO_2$	batch	[7]
liquid	50	5	no info	no	6	−3	$CH_4 + CO_2$	batch	[34]
liquid	35	280	130	no	5.4, 6.0	0	$CH_4 + CO_2$	batch	[30]
liquid	17	100	200	sand	5	8	CO_2	batch	[35]
liquid	50	300	100	sandstone	8.3	4	$CH_4 + CO_2$	batch	[36–38]
emulsion with H_2O	25	100	200	sand	5	8	CO_2	batch	[39]
supercritical	40.7/37.5	44/76	2000	sand	13/7.5	8	$CH_4 + CO_2$	flow-through	This study
supercritical	10.7	73	2000	sand	13	10	CH_4	flow-through	This study
supercritical	3.4	46	2000	sand	13	2	$CH_4 + CO_2$	flow-through	This study

Note: In the listed studies pure water as well as saline waters were used. Please refer to the references for more details.

As discussed before, this is due to immediate CO_2-hydrate formation with excess water in the pore space. A blocking of pore space by CO_2-hydrate formation resulting in low CH_4 yields was also encountered by Zunzhao *et al*. [33] and Hirohama *et al*. [7]. For similar reasons, Zhou *et al*. [39] could only achieve ~25% of hydrate conversion when applying a CO_2-H_2O emulsion.

Most of the other studies, summarized in Table 3, avoided excess water in their experiments. Nevertheless, the achieved methane yield varies over a wide range from similarly low values of 17%–27% [28–30,35] to almost 100% [27,31,32]. The main reason for this scatter is founded in very different experimental conditions, and as a consequence it is difficult to deduce an overall trend. Many of the experiments were conducted at *p-/T-* conditions close to the CH_4-water phase boundary and here it seems preferential if the injected CO_2 is gaseous [27,31,32] rather than liquid [35,39]. In two of those studies [27,32] the temperature was actually raised when introducing the CO_2 gas such that the pure CH_4-hydrates were no longer stable during the conversion reaction. Hence, the CH_4-hydrate was actively destabilized by adding heat to the system, *i.e*., in some way a similar strategy as in our experiments.

Experiments that were conducted at *p-/T-* conditions well within the stability fields of both gas hydrates [28–30,34,36–38] usually achieved only moderate hydrate conversion (Table 3). Two processes may be most likely to explain these findings: (1) Formation of mixed CH_4-CO_2-hydrates of varying composition and (2) a relatively quick gas exchange at the surface of the CH_4-hydrate grain forming a shell out of CO_2-hydrate and thereby inhibiting the further gas exchange, *i.e*., mass transport, into and out of the inner core of the hydrate grain. The latter process has been documented for the CH_4-C_2H_8 gas replacement [17] and seems very likely to occur in the above batch-type experiments. Since the overall process, particularly in a sediment/sand matrix, is quite complex, some other factors, such as local limitations in heat transfer and hydrate grain size, may also play a role (see Conclusion section for more details).

Thus, the major advantage of injecting supercritical CO_2 is the destruction of the original CH_4-hydrate excluding mass transfer limitations at hydrate grains. As a consequence, it is possible to establish a continuous production of CH_4 gas. Furthermore, immediate formation of the more stable CO_2-hydrates or mixed CO_2-CH_4-hydrates can be avoided at suitable reservoir temperatures potentially because the cooling of the CO_2 takes some time, and the liberated CH_4 gas warms up and migrates towards the outlet in the equilibration periods of our experiment.

5. Conclusions

In this study we presented the first experimental results on CH_4 production from CH_4-hydrates by injection of hot, supercritical CO_2. Based on the inventories of the components CO_2, CH_4, and H_2O (Table 4) the overall process performance was analyzed with respect to CH_4 production, CO_2 and H_2O retention as well as energy efficiency (Table 5). The central finding of this study is that continuous CH_4 production can be achieved, if some initial heat is introduced together with the CO_2. The hot, supercritical CO_2 efficiently activates the CH_4-hydrate reservoir and thereby overcomes mass transport limitations typically observed with cold CO_2. However, the reservoir temperature also plays a crucial role and definitely needs consideration when developing an exploitation strategy. At cold temperatures, rapid cooling of the injected CO_2 can induce formation of CO_2-hydrate with excess water causing congestions in the fluid pathways that may lead to complete process failure. We could

further show that both, CH_4 production and CO_2 retention is improved under conditions of slow CO_2-hydrate formation. Constant CH_4 production efficiencies at all temperatures indicate that production is driven by fast thermal destabilization of CH_4-hydrates rather than by slow hydrate conversion. Surprisingly, the combination of mass flow analysis, volume and energy balancing suggests that CH_4 production is limited by gas mobilization rather than by CH_4-hydrate dissociation. Overall, it seems to be necessary to consider secondary processes for the overall CH_4 production process.

Table 4. Component inventories and phase distribution. Initial and final component and phase inventories are shown. Final amounts of components n_{final} were calculated from mass balance analysis. Amounts of gaseous CH_4 in the pressure vessel were estimated from volume differences. However, $n_{CH4,g}$ is putatively underestimated in cases of rapid CO_2-hydrate formation, and overestimated if CH_4-hydrate reformation occurs. Final hydrate inventories $n_{CH4,hyd}$ and $n_{CO2,hyd}$ are calculated from component inventories and show maximum values.

No.	T, p	CH_4				CO_2				H_2O	
		$n_{Initial}$ /mol	n_{Final} /mol	$n_{CH4,hyd}$ /mol	$n_{CH4,g}$ /mol	$n_{Initial}$ /mol	n_{Final} /mol	$n_{CO2,hyd}$ /mol	$n_{CO2,inj}$ /mol	$n_{Initial}$ /g	n_{Final} /g
1	**2 °C, 13 MPa**	2.9	2.8	2.1–2.8	<0.7	0	17.0	<7.7	21.9	1452	804
2	**8 °C, 13 MPa**	2.7	1.6	1.4–1.6	< 0.2	0	16.0	<8.3	27.5	1495	860
3	**10 °C, 13 MPa**	2.8	2.5	0.4–2.5	< 2.1	0	9.1	<8.4	21.6	1429	871
4	**8 °C, 8 MPa**	2.4	1.5	1.4–1.5	< 0.1	0	12.5	<7.5	21.5	1395	779

Table 5. Summary of results: Mass and energy based process efficiencies and yields.

No.	T, p	CH_4			CO_2			H_2O		Energy	
		Y_{CH4}		E_{CH4}	S_{CO2}		E_{CO2}	S_{H2O}		$E_{\Delta H,prod}$	$E_{\Delta H,rel}$
		/mol	/mol-%		/mol	/mol-%		/g	/w-%	/J-%	/J-%
1	**2 °C, 13 MPa**	0.1	2.4	0.003	17.1	77.9	0.78	804	55	2.4	18.3
2	**8 °C, 13 MPa**	0.8	31.2	0.030	16.0	58.0	0.58	860	58	19.4	23.2
3	**10 °C, 13 MPa**	0.4	12.5	0.016	9.1	42.5	0.43	871	61	8.2	57.4
4	**8 °C, 8 MPa**	0.8	35.5	0.039	12.5	58.0	0.58	779	56	17.6	21.0

The combination of CH_4 extraction from gas hydrates and storage of CO_2 results in a complex multi-component, multiphase transport-reaction scheme, as illustrated in Figure 9. Highly dynamic processes on different time scales are putatively important for CH_4-hydrate dissociation, hydrate conversion and pure or mixed hydrate reformation, all of them altering sediment parameters, such as bulk thermal and geomechanical behavior. Due to the spatial heterogeneity and concurrency of multiple processes, it is very likely that optimization efforts will be most successful when considering processes down to the pore scale. This underlines the technical relevance of former studies of CH_4-CO_2-hydrate conversion (Table 3), hydrate dissociation and formation ([40] and references therein), which were strongly focused on gaining mechanistic insights on grain size and molecular scale.

Figure 9. Process dynamics scheme. Relevant transport and reaction processes during injection of hot $CO_{2,sc}$ into CH_4-hydrate bearing sediment. (1) Injection of hot, mobile $CO_{2,sc}$; (2) Fast dissociation of CH_4-hydrate due to thermal stimulation from hot $CO_{2,sc}$ injection; (3) Conductive heat transport via sediment particles or non-mobile pore water followed by thermal stimulation and dissociation of distant CH_4-hydrate particles; (4) Mixing of CO_2 and CH_4; (5) CO_2-hydrate formation with pore water; (6) Formation of mixed CO_2-CH_4-hydrates from CO_2-CH_4 gas mixtures; (7) CH_4-CO_2-hydrate exchange limited by diffusive transport of CH_4 and CO_2; (8) $CO_{2,sc}$ cools and rapidly transforms to $CO_{2,liq}$. CO_2-CH_4 mixtures remain supercritical at high CH_4 content; (9) CO_2-hydrate formation with excess pore water might result in pore space clogging followed by substantial change of porosity and permeability. Complete loss of hydraulic conductivity is possible; (10) Production of fluid containing CH_4, water and CO_2 in various states and different and changing proportions; (11) Dissociation of load-bearing hydrate particles can cause settling of sediment and change of sediment integrity and geomechanical stability; (12) CH_4 gas might be released into hydraulically isolated pores as non-producible gas.

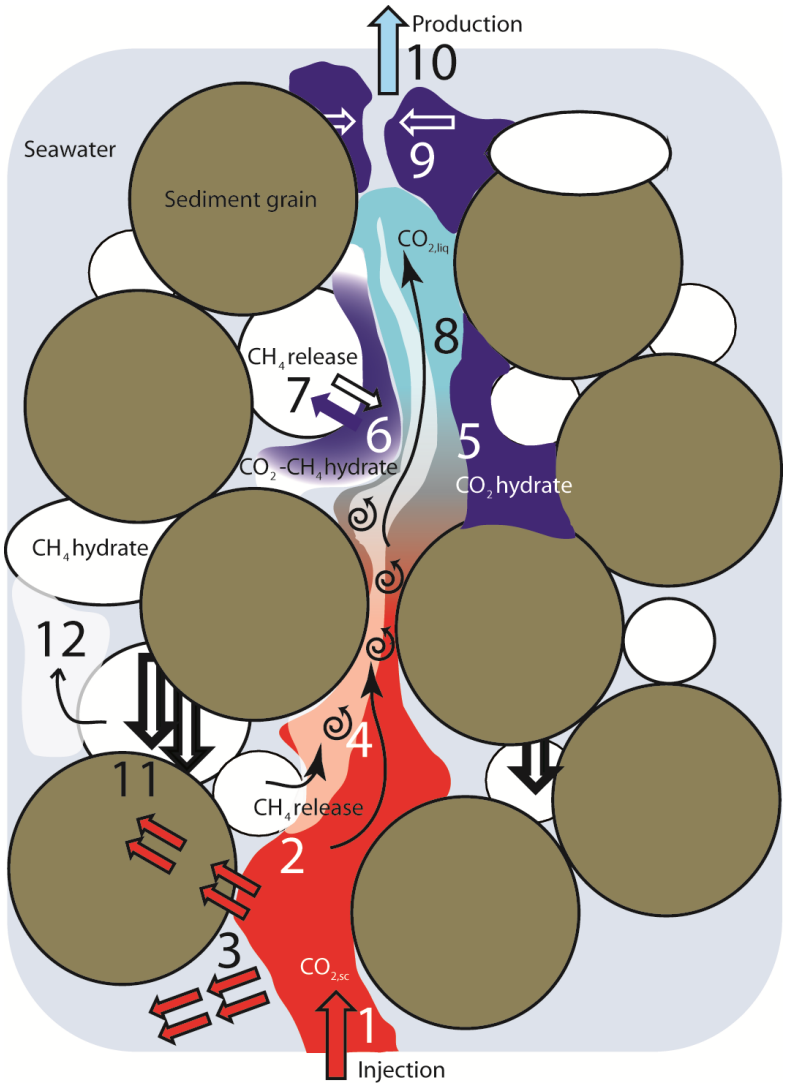

6. Outlook

Our results suggest that both efficiency and rate of CH_4 production can be optimized in numerous ways.

The additional combination with depressurization is likely to improve the production process, since CH_4-hydrates could initially be destabilized to facilitate injection of the supercritical CO_2. In turn, the heat of the CO_2 can then compensate the cooling of the reservoir induced by the endothermic hydrate dissociation from depressurization. As a consequence, substantial production rates of CH_4 gas could be maintained over extended periods of time.

Different modifications of the injection fluid with respect to its composition and injection temperature as well as of the injection strategy itself might avoid early CO_2 breakthrough and also improve gas mobilization, which was identified as a possible obstacle in the production process (*i.e.*, in the 10 °C experiment).

According to our results, reservoir conditions including temperature, pressure and permeability have a major influence on the production process and the choice of appropriate reservoir sites and technical means to influence the reservoir properties will be of paramount importance. So far, our experiments lack from the impossibility to directly monitor the processes and phase distribution inside the pressure vessel. Instead, this information has to be obtained indirectly from the analysis of effluent fluids. Hence, future studies would benefit significantly from the application of online monitoring including imaging techniques such as MRI or CT.

Because of the complexity of the numerous physical and chemical processes contributing to the overall CH_4 production we emphasize the importance of understanding the behavior of the system from the reservoir scale down to the pore scale. Only such knowledge can lead to progress in production simulations and laboratory experiments, which are prerequisites for the development of optimized production techniques.

Acknowledgments

The authors would like to thank the colleagues at the FH Kiel for constructing and building NESSI as well as CONTROS GmbH for developing a custom-made data acquisition system. This work was funded by the German Ministry of Economy (BMWi) through the SUGAR project (grant No. 03SX250 & 03SX320A) and by RWE Dea AG and Wintershall Holding AG through the project CLATHRAT.

References

1. Kvenvolden, K.A.; Lorenson, T.D. A Global Inventory of Natural Gas Hydrate Occurrence. Available online: http://walrus.wr.usgs.gov/globalhydrate/ (accessed on 9 May 2012).
2. Archer, D.; Buffett, B.; Brovkin, V. Ocean methane hydrates as a slow tipping point in the global carbon cycle. *Proc. Nat. Acad. Sci. USA* **2009**, *106*, 20596–20601.
3. Burwicz, E.B.; Rüpke, L.H.; Wallmann, K. Estimation of the global amount of submarine gas hydrates formed via microbial methane formation based on numerical reaction-transport modeling and a novel parameterization of holocene sedimentation. *Geochim. Cosmochim. Acta* **2011**, *75*, 4562–4576.

4. Gornitz, V.; Fung, I. Potential distribution of methane hydrates in the world's oceans. *Global Biogeochem. Cycle* **1994**, *8*, 335–347.
5. Kvenvolden, K.A. Gas hydrates, geological perspective and global change. *Rev. Geophys.* **1993**, *31*, 173–187.
6. Moridis, G.J.; Collett, T.S.; Boswell, R.; Kurihara, M.; Reagan, M.T.; Koh, C.; Sloan, E.D. Toward production from gas hydrates: Current status, assessment of resources, and simulation-based evaluation of technology and potential. *Soc. Petrol. Eng. J.* **2008**, *114163*, 1–43.
7. Hirohama, S.; Shimoyama, Y.; Wakabayashi, A.; Tatsuta, S.; Nishida, N. Conversion of CH_4-hydrate to CO_2-hydrate in liquid CO_2. *J. Chem. Eng. Jpn.* **1996**, *29*, 1014–1020.
8. Ohgaki, K.; Takano, H.; Sangawa, H.; Matsubara, T.; Nakano, S. Methane exploitation by carbon dioxide from gas hydrates-phase equilibria for CO_2-CH_4 mixed hydrate systems. *J. Chem. Eng. Jpn.* **1996**, *29*, 478–483.
9. Dallimore, S.R.; Collett, T.S. *Scientific Results from the Mallik 2002 Gas Hydrate Production Research Well Program*, *Mackenzie Delta*, *Northwest Territories*, *Canada*, 1st ed.; Geological Survey of Canada: Ottawa, Canada, 2005.
10. Yamamoto, K.; Dallimore, S. Aurora-jogmec-nrcan mallik 2006–2008 gas hydrate research project progress. *Fire Ice* **2008**, *Summer*, 1–5.
11. Schoderbek, D.; Boswell, R. Ignik sikumi #1, gas hydrate test well, successfully installed on the alaska north slope. *Fire Ice* **2011**, *11*, 1–5.
12. Masuda, Y.; Yamamoto, K.; Tadaaki, S.; Ebinuma, T.; Nagakubo, S. Japan's methane hydrate R&D program progresses to phase 2. *Fire Ice* **2009**, *9*, 1–6.
13. Nagakubo, S.; Arata, N.; Yabe, I.; Kobayashi, R.; Yamamoto, K. Environmental impact assessment study on japan's methane hydrate R&D program. *Fire Ice* **2011**, *11*, 4–11.
14. Konno, Y.; Masuda, Y.; Hariguchi, Y.; Kurihara, M.; Ouchi, H. Key factors for depressurization-induced gas production from oceanic methane hydrates. *Energy Fuels* **2010**, *24*, 1736–1744.
15. Moridis, G.J.; Silpngarmlert, S.; Reagan, M.T.; Collett, T.; Zhang, K. Gas production from a cold, stratigraphically-bounded gas hydrate deposit at the mount elbert gas hydrate stratigraphic test well, alaska north slope: Implications of uncertainties. *Mar. Petrol. Geol.* **2011**, *28*, 517–534.
16. Dornan, P.; Alavi, S.; Woo, T.K. Free energies of carbon dioxide sequestration and methane recovery in clathrate hydrates. *J. Chem. Phys.* **2007**, *127*, 124510:1–124510:8
17. Murshed, M.M.; Schmidt, B.C.; Kuhs, W.F. Kinetics of methane-ethane gas replacement in clathrate-hydrates studied by time-resolved neutron diffraction and raman spectroscopy. *J. Phys. Chem. A* **2010**, *114*, 247–255.
18. NETL. The National Methane Hydrates R&D Program. Available online: http://www.netl.doe.gov/technologies/oil-gas/FutureSupply/MethaneHydrates/rd-program/ANSWell/co2_ch4exchange.html (accessed on 25 June 2012).
19. Chen, P.-C.; Huang, W.-L.; Stern, L.A. Methane hydrate synthesis from ice: Influence of pressurization and ethanol on optimizing formation rates and hydrate yield. *Energy Fuels* **2010**, *24*, 2390–2403.
20. Stern, L.A.; Circone, S.; Kirby, S.H.; Durham, W.B. Temperature, pressure, and compositional effects on anomalous or "Self" Preservation of gas hydrates. *Can. J. Phys.* **2003**, *81*, 271–283.

21. Berges, J.A.; Franklin, D.J.; Harrison, P.J. Evolution of an artificial seawater medium: Improvements in enriched seawater, artificial water over the last two decades. *J. Phycol*. **2001**, *37*, 1138–1145.
22. Tishchenko, P.; Hensen, C.; Wallmann, K.; Wong, C.S. Calculation of the stability and solubility of methane hydrate in seawater. *Chem. Geol.* **2005**, *219*, 37–52.
23. Tishchenko, P.Y.; Wong, C.S.; Johnson, W.K.; Haeckel, M.; Wallmann, K.; Aloisi, G. Stability and solubility of CO_2 hydrate in seawater. In *Proceedings of 8th International Carbon Dioxide Conference*, Jena, Germany, 13–19 September 2009.
24. Span, R.; Wagner, W. A new equation of state for carbon dioxide covering the fluid region from the triple-point temperature to 1100 k at pressures up to 800 mpa. *J. Phys. Chem. Ref. Data* **1996**, *25*, 1509–1596.
25. Setzmann, U.; Wagner, W. A new equation of state and tables of thermodynamic properties for methane covering the range from the melting line to 625 k at pressures up to 100 mpa. *J. Phys. Chem. Ref. Data* **1991**, *20*, 1061–1155.
26. Seo, Y.-T.; Lee, H. Multiple-phase hydrate equilibria of the ternary carbon dioxide, methane, water mixtures. *J. Phys. Chem.* **2001**, *B105*, 10084–10090.
27. Komai, T.; Yamamoto, Y.; Ohga, K. Dynamics of reformation and replacement of CO_2 and CH_4 hydrates. *Ann. N. Y. Acad. Sci.* **2000**, *912*, 272–280.
28. Ota, M.; Abe, Y.; Watanabe, M.; Smith, R.L.; Inomata, H. Methane recovery from methane hydrate using pressurized CO_2. *Fluid Phase Equilibria* **2005**, *228–229*, 553–559.
29. Ota, M.; Morohashi, K.; Abe, Y.; Watanabe, M.; Smith, R.L.; Inomata, H. Replacement of CH_4 in the hydrate by use of liquid CO_2. *Energy Convers. Manag.* **2005**, *46*, 1680–1691.
30. Ota, M.; Saito, T.; Aida, T.; Watanabe, M.; Sato, Y.; Smith, R.L.; Inomata, H. Macro and microscopic CH_4-CO_2 replacement in ch_4 hydrate under pressurized CO_2. *Am. Inst. Chem. Eng. J.* **2007**, *53*, 2715–2721.
31. Park, Y.; Kim, D.-Y.; Lee, J.-W.; Huh, D.-G.; Park, K.-P.; Lee, J.; Lee, H. Sequestering carbon dioxide into complex structures of naturally occurring gas hydrates. *Proc. Nat. Acad. Sci. USA* **2006**, *103*, 12690–12694.
32. Yoon, J.-H.; Kawamura, T.; Yamamoto, Y.; Komai, T. Transformation of methane hydrate to carbon dioxide hydrate: *In situ* raman spectroscopic observations. *J. Phys. Chem. A* **2004**, *108*, 5057–5059.
33. Li, Z.; Guo, X.; Yang, L.; Ma, X. Exploitation of methane in the hydrate by use of carbon dioxide in the presence of sodium chloride. *Petrol. Sci.* **2009**, *6*, 426–432.
34. Lee, H.; Seo, Y.; Seo, Y.-T.; Moudrakovski, I.L.; Ripmeester, J.A. Recovering methane from solid methane hydrate with carbon dioxide. *Angew. Chem. Int. Ed.* **2003**, *42*, 5048–5051.
35. Zhou, X.; Fan, S.; Liang, D.; Du, J. Determination of appropriate condition replacing methane from hydrate with carbon dioxide. *Energy Convers. Manag.* **2008**, *49*, 2124–2129.
36. Ersland, G.; Husebø, J.; Graue, A.; Baldwin, B.A.; Howard, J.; Stevens, J. Measuring gas hydrate formation and exchange with co_2 in bentheim sandstone using mri tomography. *Chem. Eng. J.* **2010**, *158*, 25–31.

37. Graue, A.; Kvamme, B.; Baldwin, B.A.; Stevens, J.; Howard, J.; Aspenes, E.; Ersland, G.; Husebø, J.; Zornes, D. Environmentally friendly CO_2 storage in hydrate reservoirs benefits from associated spontaneous methane production. In *Proceeding of Offshore Technology Conference*, Houston, TX, USA, 2006.
38. Kvamme, B.; Graue, A.; Buanes, T.; Kuznetsova, T.; Ersland, G. Storage of CO_2 in natural gas hydrate reservoirs and the effect of hydrate as an extra sealing in cold aquifers. *Int. J. Greenhouse Gas Control* **2007**, *1*, 236–246.
39. Zhou, X.; Fan, S.; Liang, D.; Du, J. Replacement of methane from quartz sand-bearing hydrate with carbon dioxide-in-water-emulsion. *Energy Fuels* **2008**, *22*, 1759–1764.
40. Sloan, E.D.; Koh, C.A. *Clathrate Hydrates of Natural Gases*, 3rd ed.; Marcel Dekker, Inc.: New York, NY, USA, 2007; p. 705.